Strong earthquake-prone areas recognition based on the algorithm with a single pure training class. II. Caucasus, $M \geq 6.0$. Variable EPA method

B. A. Dzeboev[1,2], A. A. Soloviev[3], B. V. Dzeranov[2], J. K. Karapetyan[4], and N. A. Sergeeva[1]

Strong earthquake-prone areas recognition ($M \geq 6.0$) in the Caucasus is performed by means of the new "Barrier-3" pattern recognition algorithm. The obtained result is compared with potentially high seismicity zones recognized previously using the "Cora-3" pattern recognition algorithm. It is proposed to define an interpretation of the integral recognition result by the "Barrier-3" and "Cora-3" algorithms as a fuzzy set of recognition objects in the vicinity of which strong earthquakes may occur in the Caucasus. *KEYWORDS:* Earthquake-prone areas recognition; EPA; Cora-3; Barrier-3; Caucasus; seismic hazard assessment; fuzzy set.

Introduction

Strong earthquake-prone areas recognition was developed as a part of mathematical geophysics in the early 1970s in the works of academicians I. M. Gelfand and V. I. Keilis-Borok [*Gelfand et al.,* 1972, 1973, 1974, 1976]. This approach was later named EPA (Earthquake-Prone Areas recognition) [*Gvishiani et al.,* 1988; *Kossobokov and Soloviev,* 2018; *Soloviev et al.,* 2014]. It is based on the hypothesis that the epicenters of rather strong earthquakes are confined to the intersections of the morphostructural lineaments (morphostructural nodes) but not to all of them. A prob-lem (EPA problem), which is solved, is to determine in the region under consideration all high-seismicity nodes where strong earthquakes may occur. For more than 40 years, the EPA approach has been successfully used for recognition of earthquake-prone areas in various mountain countries [*Gvishiani et al.,* 1988; *Soloviev et al.,* 2014]. Its detailed description, the ideas embodied in it and the ways for its development are given in [*Gvishiani et al.,* 1988; *Kossobokov and Soloviev,* 2018; *Soloviev et al.,* 2014].

Pattern recognition algorithms with training "Cora-3", "Subclasses", "Hamming", etc. are used in the EPA approach [*Gvishiani et al.,* 1988]. They require the a priori formation of training samples of high- and low-seismicity classes that are used at the learning stage of algorithm application. The most commonly used algorithm in EPA is "Cora-3" [*Bongard et al.,* 1966]. The result of the pattern recognition in the EPA approach [*Gvishiani et al.,* 1988] is twofold: (1) the rule of recognition and (2) the actual division of objects (morphostructural nodes) into two separate classes (high and low seismicity objects). Actually the recognition rule contains a geological-geophysical and geomorphologi-

---

[1]Geophysical Center RAS, Moscow, Russia

[2]Geophysical Institute, Affiliate of Vladikavkaz Science Center RAS, Vladikavkaz, Russia

[3]Institute of Earthquake Prediction Theory and Mathematical Geophysics RAS, Moscow, Russia

[4]Institute of Geophysics and Engineering Seismology after A. Nazarov, Gyumri, Armenia

cal description of these classes, i.e. criteria of high and low seismicity for the considered region.

As shown in [*Dzeboev et al.,* 2019; *Gvishiani et al.,* 2017a] the training samples of the high and low seismicity classes have different levels of confidence, but this was ignored when a pattern recognition algorithm is applied in the EPA approach. That is a disadvantage of the approach and the "Barrier" algorithm [*Gvishiani et al.,* 2017a] has been developed to avoid it. This algorithm requires only a high seismicity class training sample, which is a reliable one.

The purpose of the "Barrier" algorithm is to study the characteristics of the "pure" training sample of the high-seismicity class and to identify on this basis among the whole set of objects those that are "similar" to objects from the training sample. In the language of set theory "Barrier" solves the problem of constructing in the finite set of objects its subset, which is extension of the only one reliable training sample of the high seismicity class.

Initially, the "Barrier" algorithm has been successfully applied to recognition of strong (with $M \geq 6.0$) earthquake-prone areas in the Caucasus [*Gvishiani et al.,* 2017a]. Later the new version "Barrier-3" [*Dzeboev et al.,* 2019] has been developed on the basis of the "Barrier" algorithm. The modification consisted in the creation of computing units that allow us to estimate both the average contribution of all geological and geophysical characteristics and the contribution of the three "strongest" characteristics only. The "Barrier-3" algorithm has been successfully used for recognition of strong (with $M \geq 6.0$) earthquake-prone areas in the Altai-Sayans-Cisbaikalia region [*Dzeboev et al.,* 2019].

This paper does not describe the "Barrier" and "Barrier-3" algorithms. The description of the mathematical construction of the "Barrier" algorithm in its initial version is given in the paper [*Gvishiani et al.,* 2017a]. The description of the computing units that led to the "Barrier-3" version of the algorithm is given in the paper [*Dzeboev et al.,* 2019].

This study is devoted to application of the "Barrier-3" algorithm for the identification of earthquake-prone areas for $M \geq 6.0$ in the Caucasus. The difference from the research described in [*Gvishiani et al.,* 2017a] is not only in the use of "Barrier-3" but also in the set of geological-geophysical and geomorphological characteristics

that are describing recognition objects. The entire set of available geological-geophysical and geomorphological characteristics was used in [*Gvishiani et al.,* 2017a]. In our work a preliminary test of the informativity of the characteristics in the context of the separation of recognition objects into high and low seismicity classes has been performed following to [*Soloviev et al.,* 2016]. The recognition result by the "Barrier-3" algorithm is compared with the result obtained by "Cora-3" [*Soloviev et al.,* 2016].

Caucasus Region

The Caucasus is a part of the Alpine-Himalayan folded belt located between the Black and Caspian seas. It is a complex system of alpine folded structures with the latest active tectonic movements. The modern structure, geodynamics, and seismicity of the Caucasus region are determined by submeridional contraction associated with the continuing convergence of the African-Arabian and Eurasian plates of the lithosphere [*Rogozhin et al.,* 2000].

A number of longitudinal zones are distinguished in the tectonic structure of the Caucasus: the zone of the Ciscaucasia foredeeps, the meganticlinorium of the Greater Caucasus, the zone of the Transcaucasian median massifs and internal (intermountain) basins, the meganticlinorium of the Lesser Caucasus and the Middle-Araks internal (intermountain) trough. Transverse zonality is expressed in the presence of a submeridional zone of the Transcaucasian transverse uplift, crossing all longitudinal zones, and steps parallel to this zone and decreasing to the west and east of it [*Khain and Limonov,* 2004; *Milanovsky,* 1996].

Ciscaucasia occupies a vast territory that is based on the Scythian epihercynian plate. In the southern part of Ciscaucasia there are two foredeeps – Indolo-Kuban and Tersk-Caspian, separated by the Mineralovodsk saddle. These foredeeps are filled with Cenozoic sediments, the thickness of the sedimentary cover reaches 12 km, and the foundation is composed of Baikal massifs and Paleozoic folded systems. In the axial zone of the Tersko-Caspian foredeep, two large anticlines Tersk and Sunzhensk stand out. Mineralovodsk saddle lies on the axis of the Transcaucasian transverse

uplift [*Milanovsky, 1996*]. The Tersk-Caspian fore-deep is characterized by significant seismicity with shallow foci of earthquakes (2–10 km).

The Greater Caucasus is an external alpine meganticlinorium extending in the northwest-southeast direction from Taman almost to Baku. The length of the Greater Caucasus is 1300 km with a width of up to 150 km [*Khain and Limonov, 2004*]. In the main ridge heights reach 4–5 km, the highest point is the Elbrus volcano (5642 m).

The arch-block structure of the Greater Caucasus is characterized by the asymmetric structure with sharply defined axial uplift. The core, a wide northern limb relatively simple constructed, crumpled into large folds and complicated by transverse uplifts, and a narrower and more complex constructed southern limb that is characterized by compressed folds with a tendency to thrust and overturn to the south are distinguished [*Milanovsky, 1996*]. The asymmetry of the Greater Caucasus is also associated with the presence of a very narrow and steep zone of the southern slope. This slope limited on the side of intermountain troughs by the currently active thrust belt, and on the Black Sea side by the fault zone. Along this zone, seismic activity is noted. The northern slope is smoother and it is also limited by the zone of deep faults very active in contemporary times, which is manifested in increased seismicity [*Rogozhin et al., 2000*].

The Greater Caucasus has a pronounced transverse zonality. Meganticlinorium is divided by submeridional faults into three large transverse segments – Northwest, Central and Southeast. The Central segment occupies the highest position, and the other two stepwise submergence from it to the sides of the Azov-Black Sea and Caspian depressions [*Khain and Limonov, 2004*; *Milanovsky, 1968*]. Transverse disturbances in the structure of the Greater Caucasus, as a rule, are high-amplitude faults, often having a shear component [*Rogozhin et al., 2000*].

In the Central Caucasus, there is a distinct axial uplift composed of dislocated and highly metamorphosed rocks of the Proterozoic and Lower Paleozoic. This segment lies in the strip of the Transcaucasian transverse uplift.

The northwestern segment, separated from the Central by the system of Pshekh-Adler transverse deep faults is narrower and less elevated than the Central. It passes into the Taman-Kerch transverse immersion zone with long-term mud volcanism.

The southeastern segment is separated from the Central by Transcaucasian deep fault, characterized by rapid submergence in the east of the structures and the axial zone of meganticlinorium. The segment goes into the Absheron zone of transverse immersion, which is similar in many respects to Taman-Kerch. Mud volcanoes are also widespread here [*Milanovsky, 1968*; *Milanovsky and Khain, 1963*].

Transcaucasia is an intermountain zone located between the structures of the Greater and Lesser Caucasus. The Kakheti-Lechkhumi deep fault separates the meganticlinorium of the Greater Caucasus from this zone, where the Rioni and Kura intermountain troughs made up of a thick rock mass, (3–8 km) of Pliocene-Quaternary orogenic formations and separated by the Dzirula ledge are distinguished. In this ledge, the ancient Baikal and Palaeozoic basements are exposed. The troughs are expanding and deepening to the west and east pass into the Black Sea and South Caspian deep-sea basins [*Milanovsky, 1968*; *Milanovsky and Khain, 1963*]. The intermountain troughs are characterized by a complex modern structure, the presence of young folding and young shear disturbances [*Rogozhin et al., 2000*].

The Lesser Caucasus is an internal meganticlinorium of the alpine region. This is a complex system of ridges, volcanic uplands, and plateaus. The length of the Lesser Caucasus is about 600 km, the height of the peaks is up to four kilometers, the highest peak is Mount Aragats (4090 m). In plain view, the Lesser Caucasus is represented by a wide (150–200 km) arc convex to the north with inflection to the south of the Dzirula ledge, i.e. in the zone of the Transcaucasian transverse uplift. According to tectonic structure, the Lesser Caucasus differs from the meganticlinorium of the Greater Caucasus by the absence of a main axial ridge, several anticlinoria and synclinoria with a relatively simple folded structure stand out [*Milanovsky, 1968*]. This meganticlinorium is characterized by echelon-like uplifts substituting each other with an upward amplitude of up to 3.5 km, although on average they are smaller. In the Lesser Caucasus, the latest movements are most evident in the western and northwestern parts, within Lake Sevan and to the west. This area is characterized

by increased seismicity [*Rogozhin et al., 2000*].

The meganticlinorium of the Lesser Caucasus is bounded from the south by a narrow Middle-Araks intermountain trough. The foundation of the basin is submerged to a depth of 5 km, the cover is composed of Eocene-Neogene molasses with interbeds of young lavas.

The modern appearance of the Caucasus was formed at the latest (late orogenic) stage of tectonic development, covering a period of about the last 10 million years. This period is characterized by a significant intensification of tectonic movements and volcanic activity. At this stage, due to the increasing role of upward movements, powerful mountain structures (meganticlinoria) arose. The deepening and expansion of foredeeps and intermountain depressions took place. Regions that have experienced stable recent uplifts include two large longitudinal zones – the structures of the Greater and Lesser Caucasus. The stable submergences include the Azov and Black Sea Depressions in the west and the South Caspian Depression and the western part of the Middle Caspian in the east. Significant changes in the direction of vertical tectonic movements occurred in the rest of the Caucasus; in some cases, the sign of movements changed several times. The folding processes took place in the zones of marginal and intermountain depressions and some parts of the Greater and Lesser Caucasus. The uplift was accompanied by active movements in the zones of deep faults and a significant outburst of volcanism mainly in the zone of the Transcaucasian transverse fault and its ruptures [*Milanovsky, 1977*].

At the present stage, the tectonic development of the Caucasus continues. The lifting of the Greater and Lesser Caucasus, the submergence of troughs, the growth of folds and the movement along deep faults continue, as evidenced by the significant scope of modern movements and the significant seismicity of the Caucasus.

Repeated leveling in the Caucasus allowed us to establish not only the direction but also the rates of tectonic movements. In the Greater and Lesser Caucasus, the rate of uplift is up to 10 mm/year or more and the subsidence rate (in the troughs) up to 6 mm/year, but the nature of the velocity distribution is different. Platform areas are generally more stable – average velocities rarely exceed 2 mm/year [*GUGK, 1986*; *Zakharov, 2006*].

In general, the Caucasus mountain structures are characterized by an increase in the intensity and contrast of modern vertical movements from west to east. Movement speeds, reaching 0–2 mm/year in the Western Caucasus, increase in the axial zone of the Central Caucasus to 10–13 mm/year. From west to east, towards the activated areas, the gradients of modern vertical movements, intensity, density, frequency and depth of earthquakes also increase [*Lilienberg and Shirinov, 1977*].

For the central sector of the Greater Caucasus meganticlinorium, there is a difference in the direction of modern horizontal surface movements according to measurements by satellite geodesy (GPS) [*Prilepin et al., 1997*]. Given the general tendency for the measurement points to move northward in Transcaucasia and on the northern slope of the mountain-folding structure of the Greater Caucasus, there are several places on the southern slope where movements to the south are recorded [*Rogozhin et al., 2015*].

The results of geodynamic research in the Caucasus region using GPS technology in 1991–1994 showed the existence of rapid horizontal movement of the Miskhan-Zangezur middle massif of the Lesser Caucasus relative to the motionless North-Caucasian marginal massif to the north. It was also established that the displacement rates of the mobile system of the Lesser Caucasus relative to the North Caucasus marginal massif decrease from south to north and from east to west, which can be interpreted as an uneven horizontal reduction of the mountainous region in the various parts of Caucasus [*Rogozhin et al., 2000*].

The nature of modern movements in the Caucasus region largely determines its seismic activity and the location of the strongest earthquake sources. The greatest concentration of earthquake epicenters and their maximum intensity correspond to the conjugation areas of the latest structures with movements of various signs (uplifts and subsidences). The epicenters of earthquakes are confined to the boundaries of the uplift and relative subsidence regions (foothills, intermountain and foothill troughs) which have both a general Caucasian and a meridional direction. The Transcaucasian transverse uplift is a zone of increased seismic activity. Within this uplift the main strong earthquakes of the Caucasus are concentrated.
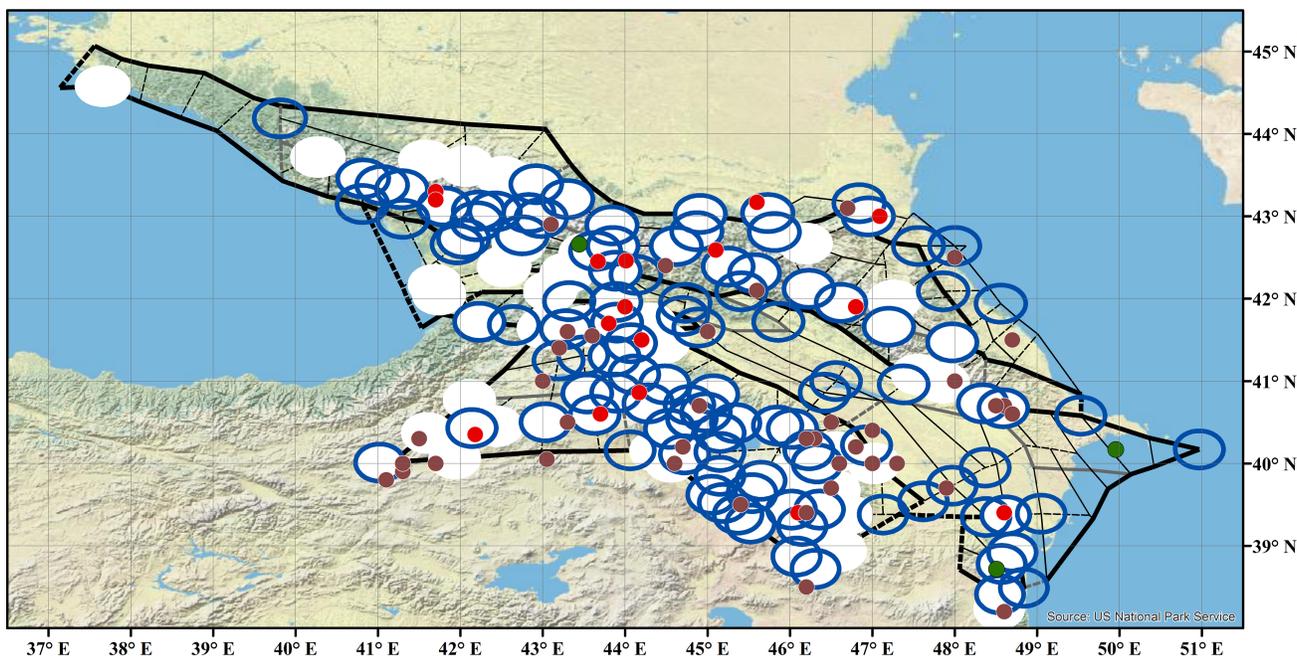
Figure 1. Scheme of morphostructural zoning (thick lines – lineaments of the I rank, medium – II rank, thin – III rank, solid lines – longitudinal lineaments, dashed – transverse lineaments [*Soloviev et al., 2013*]), earthquake-prone zones with $M \geq 6.0$ (empty ellipses with blue borders – zones recognized by the "Barrier-3" algorithm, white ellipses – "Cora-3", white ellipses with blue borders – both algorithms) and the epicenters of crustal earthquakes with $M \geq 6.0$ occurred in the Caucasus (Table 1 and Table 3) before 1900 (brown circles), in 1900–1992 (red circles), and after 1992 (green circles).

Earthquake-Prone Areas in the Caucasus, $M \geq 6.0$

Morphostructural nodes or intersections of morphostructural lineaments [*Gvishiani et al., 1988*] are considered as recognition objects in the application of the "Barrier-3" algorithm, as well as in the framework of the EPA approach. They are determined as a result of the morphostructural zoning [*Alekseevskaya et al., 1977*; *Ranzman, 1979*].

In papers [*Gvishiani et al., 1986, 1987b*; *Soloviev et al., 2013, 2016*], a scheme of the morphostructural leneaments has been constructed for the Caucasus. The scheme highlights 237 intersections of the morphostructural lineaments (Figure 1). An analysis of the positions of earthquake epicenters with $M \geq 6.0$ (Table 1) versus to the intersections of morphostructural lineaments was performed in the paper [*Soloviev et al., 2013, 2016*]. The analysis shows that the epicenters of earthquakes with $M \geq 6.0$ are located in the vicinities of lineament intersections of the Caucasus.

Applying the "Barrier-3" algorithm we use as a training sample of the high seismicity class the same 16 intersections, which were used in the paper [*Soloviev et al., 2016*] for the "Cora-3" algorithm. In the 25-km vicinities of these intersections, the crustal earthquake epicenters with $M \geq 6.0$ are known for the period 1900–1992 (Table 1 and the red circles in Figure 1). The intersections of lineaments in the vicinities of which the earthquake epicenters with $5.5 \leq M < 6.0$ since 1900 or the earthquake epicenters with $M \geq 6.0$ that occurred before 1900 are known (Table 1 and the brown circles on Figure 1) were not included in the training samples for the "Cora-3" algorithm [*Soloviev et al., 2016*]. There are 150 such intersections. The remaining 71 intersections formed the training sample of the low seismicity class for the "Cora-3" algorithm [*Soloviev et al., 2016*].

Table 2 shows the initial list of geological and geophysical characteristics that are used for describing the recognition objects in the Caucasus. According to the results of evaluating the informativity of characteristics [*Soloviev et al., 2016*] it has

Table 1. Earthquakes with $M \geq 6.0$ in the Caucasus [*Kondorskaya et al.,* 1982; *Shebalin and Tatevosian,* 1997; *Godzikovskaya,* 1999]

№	Date	φ, °	λ, °	M	№	Date	φ, °	λ, °	M
1.	427	40.5	46.5	6.5	31.	11.06.1859	40.7	48.5	6.1
2.	21.07.735	39.5	45.4	7.0	32.	24.05.1861	40.0	46.6	6.6
3.	742	42.4	44.9	6.4	33.	19.12.1862	39.7	47.9	6.0
4.	27.12.893	40.0	44.6	6.4	34.	30.12.1863	38.2	48.6	6.1
5.	23.04.1088	41.4	43.2	6.0	35.	23.07.1867	40.0	47.0	6.3
6.	1122	40.3	46.3	6.1	36.	25.02.1868	41.0	43.0	6.2
7.	28.11.1132	40.5	43.5	6.0	37.	18.03.1868	40.2	46.8	6.3
8.	30.09.1139	40.3	46.2	7.7	38.	28.01.1872	40.6	48.7	6.0
9.	07.1192	40.7	48.6	6.1	39.	01.11.1875	39.8	41.1	6.1
10.	10.1235	40.4	47.0	6.3	40.	26.06.1889	42.5	48.0	6.1
11.	17.04.1283	41.6	43.3	6.8	41.	22.09.1896	41.6	45.0	6.3
12.	1308	39.4	46.2	6.1	42.	31.12.1899	41.55	43.6	6.3
13.	1350	42.9	43.1	6.5	43.	13.02.1902	40.7	48.5	6.9
14.	29.11.1406	39.7	46.5	7.0	44.	21.10.1905	43.3	41.7	6.4
15.	1605	40.5	43.3	6.1	45.	12.10.1912	41.5	44.2	6.3
16.	1622	38.5	46.2	6.2	46.	20.02.1920	41.9	44.0	6.2
17.	1660	40.0	41.3	6.5	47.	19.02.1924	39.4	48.6	6.6
18.	14.01.1668	41.0	48.0	7.8	48.	27.04.1931	39.4	46.1	6.2
19.	11.01.1671	41.5	48.7	6.2	49.	01.05.1935	40.6	43.7	6.2
20.	04.06.1679	40.2	44.7	6.4	50.	07.05.1940	41.7	43.8	6.0
21.	1688	40.3	41.5	6.5	51.	29.06.1948	41.9	46.8	6.1
22.	08.07.1718	40.3	41.5	6.5	52.	16.07.1963	43.2	41.7	6.4
23.	05.08.1742	42.1	45.6	6.8	53.	14.05.1970	43.0	47.09	6.6
24.	10.1779	40.3	41.5	6.5	54.	28.07.1976	43.17	45.6	6.2
25.	20.10.1827	40.7	44.9	6.5	55.	30.10.1983	40.35	42.18	6.8
26.	09.03.1830	43.1	46.7	6.8	56.	07.12.1988	40.86	44.17	6.9
27.	09.04.1851	40.0	47.3	6.1	57.	29.04.1991	42.45	43.67	7.0
28.	24.07.1852	39.9	41.3	6.0	58.	15.06.1991	42.46	44.01	6.1
29.	21.01.1859	40.0	41.7	6.0	59.	23.10.1992	42.59	45.1	6.5
30.	02.06.1859	40.0	41.3	6.4					

been decided in the case of one training class [*Dzeboev et al.,* 2019] to use 11 characteristics (Table 2) when the "Barrier-3" algorithm is applied. According to the results of evaluating the informativity of characteristics for two training classes, 14 characteristics (Table 2) were used in recognition by the "Cora-3" algorithm [*Soloviev et al.,* 2016]. Note that 8 characteristics (Table 2) were used in recognition by the both algorithms. They are: maximum ($H_{\max}$), minimum ($H_{\min}$) heights and their difference ($dH = H_{\max} - H_{\min}$), combination of relief types (Top), area of Quaternary sediments (Q), number of lineaments in the vicinity of the inter-

section (NLC), distance to the closest lineament of rank II (R2) and the difference between maximum and minimum of the Bouguer anomaly (dB). To reproduce the result and enhance its reliability, the values of the characteristics of recognition objects (Table 2) are calculated by means of an intelligent GIS [*Nikolov et al.,* 2015; *Soloviev et al.,* 2018a], developed at the Geophysical Center of the Russian Academy of Sciences. This facilitates reproducing the result and enhancing its reliability.

Circles with a radius of 25 km with centers in relevant intersections of lineaments were taken in the capacity of vicinities of the recognition objects in-

Table 2. The Initial List of Geological-Geophysical and Geomorphological Characteristics of Recognition Objects in the Caucasus

Characteristics		Algorithm
Maximum height	$H_{\max}$	"Barrier-3", "Cora-3"
Minimum height	$H_{\min}$	"Barrier-3", "Cora-3"
The range of heights	$dH = H_{\max} - H_{\min}$	"Barrier-3", "Cora-3"
Height gradient	dH/l	
The combination of relief types	Top	"Barrier-3", "Cora-3"
The area of Quaternary sediments	Q	"Barrier-3", "Cora-3"
The highest rank of lineament	HR	"Barrier-3"
The number of lineaments at the intersection	NL	"Cora-3"
The distance to the nearest intersection	R_{int}	"Barrier-3"
Number of lineaments in the neighborhood of the intersection	NLC	"Barrier-3", "Cora-3"
The distance to the nearest lineament of rank I	R1	"Barrier-3"
The distance to the nearest lineament of rank II	R2	"Barrier-3", "Cora-3"
The maximum value of the Bouguer anomaly	$B_{\max}$	"Cora-3"
The minimum value of the Bouguer anomaly	$B_{\min}$	"Cora-3"
The range of the Bouguer anomaly values	$dB = B_{\max} - B_{\min}$	"Barrier-3", "Cora-3"
The maximum value of magnetic anomaly	$MO_{\max}$	"Cora-3"
The minimum value of magnetic anomaly	$HO_{\min}$	"Cora-3"
The range of the magnetic anomaly values	$MO_{\mathrm{dif}} = MO_{\max} - MO_{\min}$	"Cora-3"

side which the values of geological and geophysical characteristics are calculated. This radius corresponds to the magnitude threshold (6.0) of strong earthquakes for which potential areas of their occurrence are determined [*Gvishiani et al.,* 2017a; *Soloviev et al.,* 2013, 2016].

Empty ellipses with blue borders show in Figure 1 the result of earthquake-prone areas recognition obtained in the Caucasus for $M \geq 6.0$ by means of the "Barrier-3" algorithm. According to the result of recognition, 108 out of 237 considered recognition objects were assigned to the high seismicity class. It means that when the "Barrier-3" algorithm is used for recognition within framework of the EPA approach [*Gvishiani et al.,* 1988], the set of ellipses in Figure 1 (circles with a radius of 25 km with the centers in the corresponding 108 intersections of lineaments) shows the earthquake-prone areas for $M \geq 6.0$ in the Caucasus. It should be noted that in addition to the 16 objects from the training sample, 92 intersections of 221 are declared as high seismicity.

Figure 2 presents histograms that show the con-

tribution of 11 geological and geophysical characteristics (Table 2) in the result of recognition by the "Barrier-3" the objects, which belong to high seismicity class. Figure 2a shows for each characteristic its contribution in the recognition result that is the number of objects recognized as high seismicity, which are close according to this characteristic (in the sense of proximity embedded in the algorithm) to any object from the training sample of the high seismicity class. The numbers given in Figure 2a have been preliminarily divided by the number of objects in the training sample (16 in our case). The contribution of characteristics is described also as follows. For each characteristic the numbers of objects from the high seismicity class, which are close according to this characteristic to each object from the training sample, are calculated. Using these numbers we determine for each object from the training sample the three "strongest" characteristics according to which the largest numbers of high seismic objects are close to this object from the training sample. Figure 2b shows the numbers of objects from the training sample, for which

the characteristics fall in the triple "strongest". A detailed description of the calculation of the contribution of the characteristics is given in the paper [*Dzeboev et al.*, 2019].

It follows from Figure 2 that the greatest contribution to the formation of the high-seismicity class of objects by the "Barrier-3" algorithm is made by the characteristics, which are responsible for the relief height ($H_{\max}$ and $H_{\min}$), the area of the Quaternary sediments (Q), the highest rank of the lineament (HR), the number of lineaments in the neighborhood (NLC), as well as the distance to the nearest lineaments of the I (R1) and II (R2) ranks. The neighborhoods of the intersections of lineaments in the Caucasus, recognized by the "Barrier-3" algorithm as high seismicity for $M \geq 6.0$ are characterized against the background of the whole set of recognition objects by large values of maximum and minimum heights ($H_{\max} \geq 2500$ m and $H_{\min} \geq 600$ m), not a large area of quaternary sediments ($Q \leq 30\%$), they are formed by three or more lineaments of the II or III ranks (NLC ≥ 3, HR = 2 or HR = 3, R2 ≤ 30 km) and are located at relatively insignificant distances from the I rank lineament ($0 < $ R1 ≤ 50 km). These signs are naturally interpreted as criteria for high seismicity in the Caucasus. From Figure 2 we can see that the height range and combination of relief types also contribute to the formation of the recognition result.

White ellipses in Figure 1 show the result of earthquake-prone areas recognition obtained by means of the "Cora-3" algorithm for $M \geq 6.0$ in the Caucasus. This result is published in the paper [*Soloviev et al.*, 2016]. The total number of objects assigned to the high seismicity class is 107. They include all 16 objects from the training sample of the high seismicity class, 22 objects from a training sample of a low seismicity class, and 69 objects that were not included in the training samples. Practically all the intersections recognized by the "Cora-3" algorithm as high seismicity are associated with lineaments of the I-st and II-nd ranks. This suggests that high seismicity objects are located at the boundaries separating the largest blocks of the Earth's crust of the Caucasus [*Soloviev et al.*, 2013]. The total number of objects assigned to the high seismicity class by the "Barrier-3" algorithm is 108 and all 16 objects from the training sample of the high seismicity class are among them.

Table 3. Earthquakes With $M \geq 6.0$ in the Caucasus Since 1993

№	Date	φ, °	λ, °	M
1.	09.07.1998	38.717	48.507	6.0
2.	25.11.2000	40.167	49.954	6.5
3.	07.09.2009	42.66	43.443	6.0

A comparative analysis of the recognition results by the "Barrier-3" and "Cora-3" algorithms has been carried out. The numbers of objects that are classified as high seismicity and as low seismicity by the both algorithms are 73 and 95 respectively. The remaining 69 objects are classifiede as high seismicity by one algorithm only: 35 by the "Barrier-3" and 34 by the "Cora-3".

Denote B and C the high seismicity zones obtained by means of "Barrier-3" and "Cora-3" algorithms respectively. Figure 1 shows these zones and the differences in the recognition results obtained by the two different algorithms are observed in the western part of the Central Caucasus, on the Caspian Sea coast, and also in the southwest and southeast sectors of the considered morphostructural zoning scheme.

All 17 epicenters of earthquakes with $M \geq 6.0$ that occurred during the period 1900–1992 (Table 1 and the red circles in Figure 1) and were used for the formation of the training sample of the high seismicity class, are inside the common part $D = B \cap C$ of the zones B and C. Of the 42 epicenters of earthquakes with $M \geq 6.0$ that occurred before 1900 (Table 1 and the brown circles on the Figure 1), 7 and 8 epicenters are outside the zones B and C, respectively. Half of these epicenters are located at insignificant distances from the relevant zone and one can explain their location out of high seismicity zones by the fact that the coordinates of the earthquake epicenters that occurred before 1900 (Table 1) may be incorrect. Moreover, only one of the earthquakes with the epicenters located outside the zones B and C has a magnitude exceeding significantly 6.0 ($M = 7.8$). For all others – $6.0 \leq M \leq 6.5$ and this means that some of these earthquakes may not be the subject of study because of possible errors in magnitude.

After 1992, 3 earthquakes with $M \geq 6.0$ occurred in the studied region (Table 3 and the green circles in Figure 1). Information about these earth-
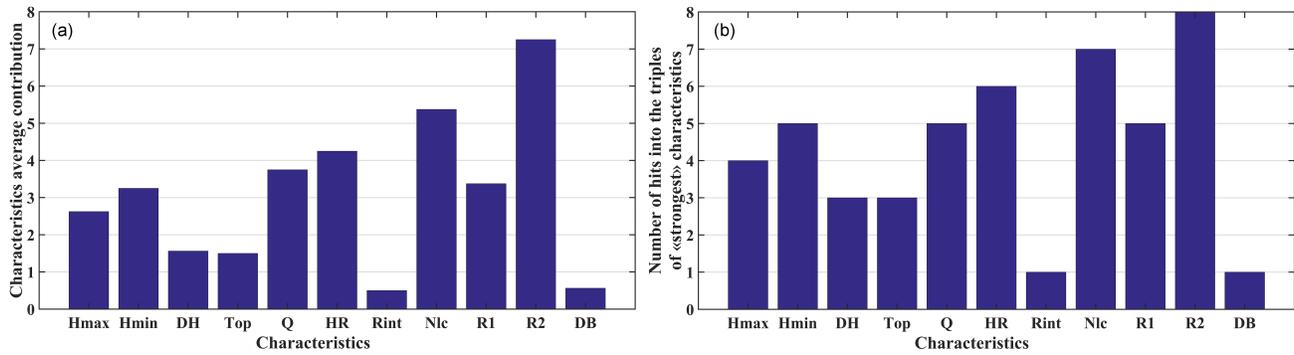
Figure 2. Recognition of high-seismicity zones ($M \geq 6.0$) in the Caucasus using the "Barrier-3" algorithm: a) the average contribution 11 geological and geophysical characteristics used in recognition; b) the contribution of the characteristics, expressed through their hit in the triples of the "strongest" characteristics.

quakes was not used in the formation of the training samples for the "Barrier-3" and "Cora-3" algorithms. An analysis of the location of their epicenters showed that two of them are located within zone D. It has to be noted that the hypocenter of the third earthquake that occurred in the Caspian Sea near the city of Baku outside the both zones B and C was according to one data, located in the crust, on others deeper – under the crust. Thus, perhaps this earthquake is not an object of our study.

Finally one can summarize that only 4 (6%) out of the 62 epicenters of earthquakes with $M \geq 6.0$ occurring since ancient times until 2018 are outside the union of the zones B and C.

An analysis of the high seismicity criteria in the Caucasus identified by the "Barrier-3" algorithm in the present work and the "Cora-3" algorithm in the paper [*Soloviev et al., 2016*] shows their sufficient proximity.

Conclusions

Applying in the EPA approach the original "Barrier-3" algorithm instead of the pattern recognition algorithms (e.g. "Cora-3") used before for dichotomy is an attempt to open a new stage in the development of this approach [*Gvishiani et al., 1988*]. According to the paper [*Gvishiani and Gurvich, 1992*], the problem of strong earthquake-prone areas recognition is a dynamic [*Dubois and Gvishiani, 1998*], limitary problem of recognition.

As shown in the paper [*Gvishiani and Gurvich, 1992*; *Gvishiani and Dubois, 2002*], in limitary problems, there is only a single reliable ("pure") training class formed by objects with which strong earthquakes that have already occurred are associated. Moreover, as a result of recognition, objects from the low seismicity training sample in the desired limitary classification may end up in a high-seismicity class.

The "Barrier-3" algorithm in its idea and construction meets more adequately than the dichotomy the dynamic problem of earthquake-prone areas recognition [*Gvishiani et al., 2017a*]. The algorithm requires the sole training sample of the high-seismicity class and determines this class by expanding the training sample.

The "Barrier-3" algorithm has proven itself in earthquake-prone areas recognition with a sole training sample in the Caucasus [*Gvishiani et al., 2017a*; and this work] and the Altai-Sayan-Baikal region [*Dzeboev et al., 2019*]. This fact strengthens our assumptions that determining the strong earthquake-prone areas by expanding their training sample is adequate for solving the EPA problem. In contrast to the FCAZ method (Formalized Clustering And Zoning) [*Gvishiani and Dzeboev, 2015*; *Gvishiani et al., 2013, 2016, 2017b*] that was also developed in the Geophysical Center of the Russian Academy of Sciences the use of "Barrier-3" does not change fundamentally the EPA approach [*Gvishiani et al., 2017a*]. In this case, only the recognition block with training changes. "Barrier-3" comes to the place of "Dichotomy algorithm", leaving the blocks of morphostructural
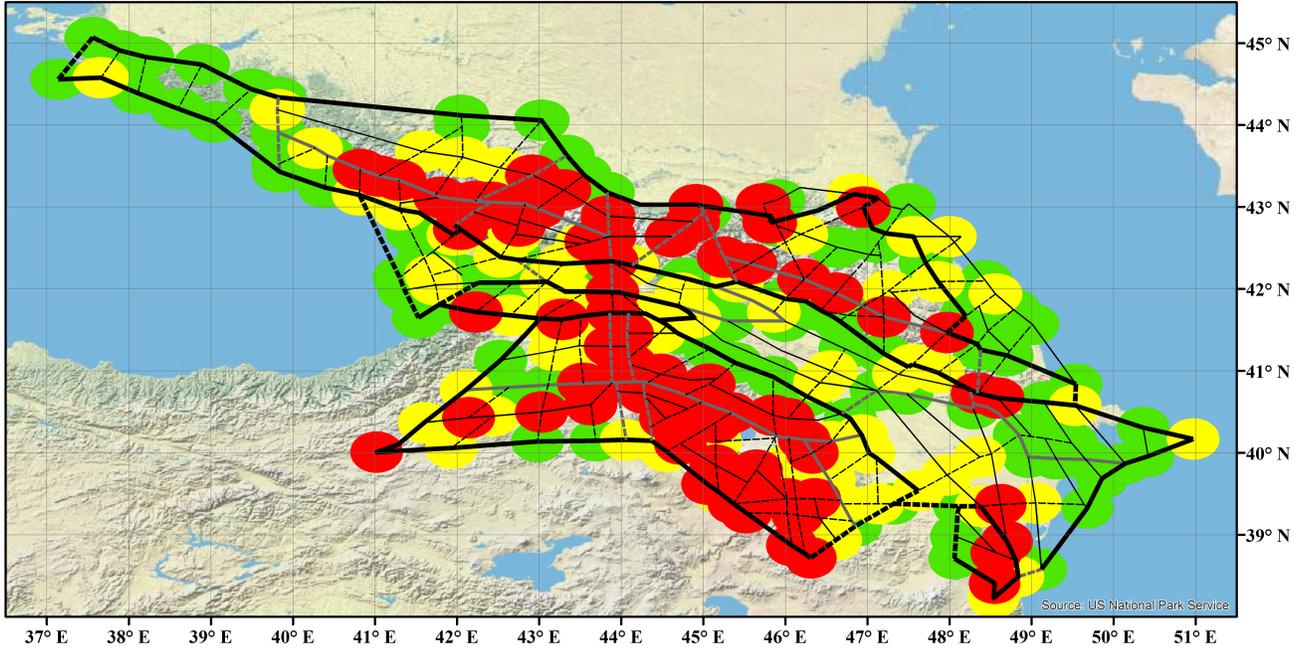
Figure 3. Presentation of integral recognition results of earthquake-prone areas recognition in the Caucasus with $M \geq 6.0$ by the "Barrier-3" and "Cora-3" algorithms as a fuzzy set of neighborhoods of lineament intersections. Red color shows neighborhoods of intersections with the membership function $\mu_{B_B,B_C} = 1$, yellow $- \mu_{B_B,B_C} = 0.5$, green $- \mu_{B_B,B_C} = 0$.

zoning and measurement of geological, geophysical and geomorphological parameters unchanged. Thus, the authors assume that the pattern recognition block in the classical EPA approach may vary: both "Dichotomy algorithm" and "Barrier-3" may be used. In the case of good consistency of both options, we can talk about the high reliability of the result.

It should be noted that the recognition results obtained independently by the "Barrier-3" and "Cora-3" algorithms are control experiments for each other. Due to the proximity of the results for Caucasus, these control experiments should be considered successful. This increases the reliability assessment of both the result of the EPA ("Dichotomy algorithm") and the EPA ("Barrier-3").

Nowadays in the Geophysical Center of the Russian Academy of Sciences under the guidance of Academician A. D. Gvishiani a project for the creation and evolving of a universal GIS-oriented database is developing [*Soloviev et al., 2018b*]. It contains solutions of a problem of strong earthquake-prone areas recognition in various regions of the world that were obtained using the EPA ("Dichotomy algorithm"), EPA ("Barrier-3")

and other methods [*Gvishiani et al., 1987a, 1988; Soloviev et al., 2014*]. Later this will make it possible to verify the universality of the variation of the pattern recognition block for other regions, where the EPA ("Dichotomy algorithm") recognition was previously successfully performed [*Soloviev et al., 2014*].

One possible interpretation of the integral recognition result by the "Barrier-3" and "Cora-3" algorithms, obtained in this paper, can be its definition as a fuzzy set $\{W, \mu_{B_B,B_C}\}$ of lineament intersections, in the neighborhood of which strong earthquakes can occur in the considered region. The corresponding membership function of such a set would have the following form:

$$\mu_{B_B,B_C}(w) =$$

$$\begin{cases} 1, & w \in B_B \cap B_C \\ 0.5, & w \in B_B \triangle B_C = (B_B \cup B_C) \backslash (B_B \cap B_C) \\ 0, & w \notin B_B \cup B_C \end{cases}$$

where $w \in W$ are the objects of recognition, and B_B, B_C are those of them, which are recognized as

high seismicity by the algorithms "Barrier-3" and "Cora-3" respectively. Figure 3 shows an example of interpreting the results of earthquake-prone areas recognition with $M \geq 6.0$ in the Caucasus in the form of a fuzzy set.

The development of the "Barrier-3" algorithm can be considered as a new step in solving the problem of strong earthquake-prone areas recognition [*Gvishiani et al.,* 1988].

References

Alekseevskaya, M., A. Gabrielov, I. Gelfand, et al. (1977), Formal morphostructural zoning of mountain territories, *Geophysics*, *42,* No. 2, 227–233.

Bongard, M. M., et al. (1966), Application of learning program for identifying oil-bearing layers, *Geol. Geofiz.*, *2,* No. 6, 15–29. (in Russian)

Dubois, J., A. Gvishiani (1998), *Dynamic Systems and Dynamic Classification Problems in Geophysical Applications*, 256 pp. Springer, Paris. **Crossref**

Dzeboev, B. A., A. D. Gvishiani, et al. (2019), Strong Earthquake-Prone Areas Recognition Based on an Algorithm with a Single Pure Training Class: I. Altai-Sayan-Baikal Region, $M \geq 6.0$, *Izvestiya, Physics of the Solid Earth*, *55,* No. 4, 563–575, **Crossref**

Gelfand, I. M., Sh. A. Guberman, et al. (1972), Criteria of high seismicity, determined by pattern recognition, *Tectonophysics*, *13,* 415–422. **Crossref**

Gelfand, I. M., Sh. A. Guberman, M. L. Izvekova, et al. Recognition of the locations of the probable occurrence of strong earthquakes. I. Pamir and Tien-Shan, *Vychislitel'naya Seismologiya*, No. 6, 107–133. (in Russian)

Gelfand, I. M., Sh. A. Guberman, et al. (1974), Recognition of the locations of the probable occurrence of strong earthquakes. III. The case when the boundaries of the disjunctive knots are unknown, *Vychislitel'naya Seismologiya*, No. 7, 41–64. (in Russian)

Gelfand, I. M., Sh. A. Guberman, et al. (1976), Pattern recognition applied to earthquake epicenters in California, *Physics of the Earth and Planetary Interiors*, *11,* No. 3, 227–283, **Crossref**

Godzikovskaya, A. A. (1999), Database "Earthquake catalogue for the Caucasus with $M \geq 4.0$ ($K \geq 11.0$) from ancient times to the year 2000" (in Russian), WDCB, Moscow. (http://zeus.wdcb.ru/wdcb/sep/caucasus/catrudat.html)

GUGK (1986), Map of modern vertical movements of the earth's crust in Bulgaria, Hungary, East Germany, Poland, Romania, the USSR (European part). Scale $1 : 10,000,000$, GUGK, Moscow.

Gvishiani, A., J. Dubois (2002), *Artificial Intelligence and Dynamic Systems for Geophysical Applications*, 350 pp. Springer-Verlag, Paris. **Crossref**

Gvishiani, A. D., B. A. Dzeboev (2015), Assessment of seismic hazard in choosing of a radioactive waste disposal location, *Mining Journal*, No. 10, 39–43, (in Russian)**Crossref**

Gvishiani, A. D., V. A. Gurvich (1992), *Dynamical Problems of Classification and Convex Programming in Applications*, 360 pp. Nauka, Moscow. (in Russian)

Gvishiani, A. D., S. M. Agayan, et al. (2017a), Recognition of Strong Earthquake–Prone Areas with a Single Learning Class, *Doklady Earth Sciences*, *474,* No. 1, 546–551, **Crossref**

Gvishiani, A., B. Dzeboev, S. Agayan (2013), A new approach to recognition of the earthquake-prone areas in the Caucasus, *Izvestiya, Physics of the Solid Earth*, *49,* No. 6, 747–766, **Crossref**

Gvishiani, A. D., B. A. Dzeboev, S. M. Agayan (2016), FCAZm intelligent recognition system for locating areas prone to strong earthquakes in the Andean and Caucasian mountain belts, *Izvestiya. Physics of the Solid Earth*, *52,* No. 4, 461–491, **Crossref**

Gvishiani, A. D., B. A. Dzeboev, N. A. Sergeyeva, A. I. Rybkina (2017b), Formalized Clustering and the Significant Earthquake-Prone Areas in the Crimean Peninsula and Northwest Caucasus, *Izvestiya. Physics of the Solid Earth*, *53,* No. 3, 353–365, **Crossref**

Gvishiani, A. D., A. I. Gorshkov, et al. (1986), Morphostructures and locations of the earthquakes of Greater Caucasus, *Izv. Akad. Nauk SSSR. Fiz. Zemli*, No. 9, 45–55. (in Russian)

Gvishiani, A., A. Gorshkov, V. Kossobokov, et al. (1987a), Identification of seismically dangerous zones in the Pyrenees, *Annales geophysicae series b-terrestrial and planetary physics*, *5,* No. 6, 681–690.

Gvishiani, A. D., A. I. Gorshkov, et al. (1987b), Recognition of the locations of probable occurrence of the strong earthquakes. XV. Morphostructural nodes of the Greater Caucasus, $M \geq 5.5$, *Vychislitel'naya Seismologiya*, No. 20, 136–148. (in Russian)

Gvishiani, A., A. Gorshkov, et al. (1988), *Recognition of Earthquake-Prone Areas in the Regions of Moderate Seismicity*, 176 pp. Nauka, Moscow. (in Russian)

Khain, V. E., A. F. Limonov (2004), *Regional geotectonics (Tectonics of Continents and Oceans)*,

270 pp. KERS, Tver. (in Russian)

Kondorskaya, N. V., N. V. Shebalin, et al. (1982), *New Catalog of Strong Earthquakes in the USSR From Ancient Times Through 1977*, 620 pp. US National Oceanic & Atmospheric Administration, Boulder, CO. (NOAA-82101304)

Kossobokov, V. G., A. A. Soloviev (2018), Pattern recognition in problems of seismic hazard assessment, *Chebyshevskii Sbornik*, *19,* No. 4, 53–88, **Crossref**

Lilienberg, D. A., N. Sh. Shirinov (1977), Contemporary tectonic movements, *General Description and History of the Relief of the Caucasus* p. 45–59, Nauka, Moscow. (in Russian)

Milanovsky, E. E. (1968), *Recent Tectonics of the Caucasus*, 483 pp. Nedra, Moscow. (in Russian)

Milanovsky, E. E. (1977), The latest tectonics, *General Description and History of the Relief of the Caucasus* p. 31–45, Nauka, Moscow. (in Russian)

Milanovsky, E. E. (1996), *Geology of Russia and the Neighboring Countries (Northern Eurasia)*, 448 pp. Moscow State University, Moscow. (in Russian)

Milanovsky, E. E., V. E. Khain (1963), *Geological Structure of the Caucasus*, Moscow State University, Moscow. (in Russian)

Nikolov, B. P., J. I. Zharkikh, A. A. Soloviev, R. I. Krasnoperov, S. M. Agayan (2015), Integration of data mining methods for earth science data analysis in GIS environment, *Russian Journal of Earth Sciences*, *15,* No. 4, ES4004, **Crossref**

Prilepin, M. T., et al. (1997), The kinematic study of the Caucasus region using GPS techniques, *Izvestiya. Physics of the Solid Earth*, *33,* No. 6, 68–75.

Ranzman, E. Ya. (1979), *Locations of the Earthquakes and Morphostructure of Mountain Regions*, Nauka, Moscow. (in Russian)

Rogozhin, E. A., A. V. Gorbatikov, et al. (2015), The structural framework and recent geodynamics of the Greater Caucasus Meganticlinorium in the light of new data on its deep structure, *Geotectonics*, *49,* No. 2, 123–134, **Crossref**

Rogozhin, E. A., V. A. Viginsky, N. A. Koronovsky (2000), Caucasus, *Latest tectonics, geodynamics and seismicity of Northern Eurasia, A. F. Grachev (ed.)* p. 66–79, Probel, Moscow. (in Russian)

Shebalin, N. V., R. E. Tatevosian (1997), Catalogue of large historical earthquakes of the Caucasus, *Historical and Prehistorical Earthquakes in the Caucasus (D. Giordini & S. Balassanian, Eds.), NATO ASI Series, 2. Enviroment – Vol. 28* p. 201–232, Kluwer Academic Publishers, Dordrecht.

Soloviev, Al. A., A. I. Gorshkov, An. A. Soloviev (2016), Application of the data on the lithospheric magnetic anomalies in the problem of recognizing the earthquake prone areas, *Izvestiya, Physics of the Solid Earth*, *52,* No. 6, 803–809, **Crossref**

Soloviev, A. A., A. D. Gvishiani, et al. (2014), Recognition of earthquake-prone areas: Methodology and analysis of the results, *Izvestiya, Physics of the Solid Earth*, *50,* No. 2, 151–168, **Crossref**

Soloviev, A. A., R. I. Krasnoperov, B. P. Nikolov, J. I. Zharkikh, S. M. Agayan (2018a), Web-Oriented Software System for Analysis of Spatial Geophysical Data Using Geoinformatics Methods, *Izvest., Atmospheric and Ocean Physics*, *54,* No. 9, 1312–1319, **Crossref**

Soloviev, A. A., O. V. Novikova, et al. (2013), Recognition of potential sources of strong earthquakes in the Caucasus region using GIS technologies, *Doklady Earth Sciences*, *450,* No. 2, 658–660, **Crossref**

Soloviev, An. A., Al. A. Soloviev, A. D. Gvishiani, B. P. Nikolov, Y. I. Nikolova (2018b), GIS-Oriented Database on Seismic Hazard Assessment for Caucasian and Crimean Regions, *Izvestiya, Atmospheric and Ocean Physics*, *54,* No. 9, 1363–1373, **Crossref**

Zakharov, V. S. (2006), Modern vertical motions of the Earth's crust, *Sovremennye Global'nye Izmeneniya Prirodnoi Sredy* p. 626–643, Nauchnyi mir, Moscow. (in Russian)

————————

Corresponding author:
B. A. Dzeboev, Geophysical Center of RAS, 3 Molodezhnaya St., 119296 Moscow, Russia. (b.dzeboev@gcras.ru)